



Cite this: *RSC Sustainability*, 2025, 3, 4435

# Improving microbial electrosynthesis with biochar electrodes in production of CO<sub>2</sub> derived biochemicals and biofuels within circular economy systems

Xue Ning, <sup>ab</sup> Deepa Sachan, <sup>ab</sup> Archishman Bose, <sup>ab</sup> David M. Wall <sup>ab</sup> and Jerry D. Murphy \*<sup>ab</sup>

The urgent need to mitigate greenhouse gas emissions and transition to a circular economy has driven the exploration of bioelectrochemical technologies including microbial electrosynthesis (MES). MES offers a promising pathway for CO<sub>2</sub> conversion into valuable biochemicals and biofuels; however, its scalability is limited by challenges such as high cathode costs, inefficient electron transfer, and poor microbial attachment. Biochar, derived from waste biomass, presents a sustainable and cost-effective alternative to conventional carbon-based electrodes due to its high porosity, tunable surface chemistry, and low associated production costs. However, the optimisation of biochar properties for MES applications, including its electrochemical performance and stability, has not been definitively analysed. This paper summarises the recent advancements in biochar electrodes for MES, focusing on material characteristics, modification strategies, and their impact on overall system efficiency. Furthermore, the potential of integrating MES with existing biogas facilities to enhance carbon recovery, and reduce resource consumption is discussed. Overcoming current challenges in consistent biochar electrode production, and its integration with existing infrastructure is essential for advancing MES technology in real world applications. The findings suggest that waste-derived biochar electrodes have the potential to improve MES scalability and economic viability, supporting the development of sustainable biochemicals within circular economy systems.

Received 27th February 2025  
Accepted 31st August 2025

DOI: 10.1039/d5su00140d

rsc.li/rscsus

<sup>a</sup>Research Ireland MaREI Centre for Energy, Climate and Marine, Sustainability Institute, Ellen Hutchins Building, University College Cork, Cork T23XE10, Ireland. E-mail: Jerry.Murphy@ucc.ie

<sup>b</sup>School of Engineering and Architecture, University College Cork, Cork T23XE10, Ireland



Xue Ning

Xue Ning will start a new role as an Assistant Professor of Bioengineering in Circular Bioeconomy in the School of Biosystems and Food Engineering in University College Dublin. She serves as a postdoctoral researcher at the MaREI Centre for Energy, Climate and Marine at University College Cork (UCC) from 2023 to 2025. She holds a PhD in energy engineering from UCC. Her early career research was on two-phase anaerobic digestion,

biogas upgrading and biochar production. She has subsequently worked on various aspects of global decarbonisation and CO<sub>2</sub> utilisation through microbial electrosynthesis. At UCC, she co-leads two national funding programmes, with focus on developing integrated bioelectrochemical systems.



Deepa Sachan

Deepa Sachan is a Post Doctoral Researcher at University College Cork (UCC), specializing in Energy Transition and Advanced Fuels in the Circular Economy. She holds a PhD in Environmental Engineering from the Indian Institute of Technology Guwahati, India. Her early career research focused on biomass-derived materials and nanomaterials synthesis for water remediation. Over time, she expanded her research into

diverse aspects of material synthesis, characterization, and environmental applications. At UCC, Deepa leads research efforts on the production and engineering of biochar and other materials derived from waste materials for emerging contaminants removal.



## Sustainability spotlight

The growing demand for sustainable energy solutions and carbon mitigation strategies underscores the need for innovative technologies to reduce greenhouse gas emissions. Microbial electrosynthesis (MES) presents a promising approach for converting CO<sub>2</sub> into valuable biochemicals and biofuels; however, its scalability is limited by high electrode material costs and inherent inefficiencies. This work advances sustainability of MES systems by developing waste-derived biochar as a cost-effective electrode, enhancing MES efficiency while promoting circular economy principles. By integrating MES with existing biogas facilities, carbon recovery and resource efficiency can be further improved. This research aligns with the UN Sustainable Development Goals (SDGs) of affordable and clean energy (SDG 7), industry, innovation, and infrastructure (SDG 9), responsible consumption and production (SDG 12), and climate action (SDG 13).

# 1 Advancing sustainable carbon utilisation through microbial electrosynthesis

An assessment of our overall impact on the environment indicates that we would need the equivalent of 1.6 times the Earth's



Archishman Bose

*Archishman Bose is an Eli Lilly Lecturer in Process and Chemical Engineering at University College Cork (UCC) and a Funded Investigator in the MaREI Centre for Energy, Climate and Marine. He has published over 20 peer reviewed journal papers on circular and bioeconomy, energy and environmental systems. His expertise and research interest includes biochemical and bioprocess engineering, process design and simulation, carbon*

*capture and utilisation, techno-economic (TEA) and life cycle assessments (LCA); circular bioeconomy systems. He is currently leading multiple nationally funded research projects and continues to research on advanced applications of biochar in energy and water applications.*



David M. Wall

*David M. Wall is an Associate Professor in the School of Engineering and Architecture at University College Cork (UCC). He is a Funded Investigator in the MaREI Centre for Energy, Climate and Marine where he has published over 50 peer reviewed journal papers on circular economy, energy and environmental systems. His research includes for innovative biogas technologies and biorefinery applications with*

*a focus on the valorisation of industry and agricultural by-products. He represents Ireland for the International Energy Agency (IEA) Bioenergy Task 37 on Biogas and is a committee member for the Irish Transport Research Network.*

resources to sustain our current global living patterns.<sup>1</sup> Raw material processing, extraction and use (including fossil fuels and metal ores) was responsible for 50% of global greenhouse gas (GHG) emissions as estimated in 2024.<sup>2</sup> The United Nations Environment Programme (UNEP) Emissions Gap Report 2020 stated that despite a reduction in GHG emissions resulting from the economic slowdown during the COVID-19 pandemic, the world is moving towards a significant temperature increase of 3 °C above pre-industrial levels within this century, well surpassing the targets set by the Paris Agreement. Increased efforts must be made to transition to a sustainable, decarbonised renewable economy driven by the challenges of climate change.

In 2023, fossil fuel-derived CO<sub>2</sub> accounted for the majority (73.7%) of total GHG emissions.<sup>3</sup> CO<sub>2</sub> emission reduction is indeed a challenge but also can lead to opportunities within a circular economy framework. Emitted CO<sub>2</sub> may be captured and converted into valuable chemicals, fuels or materials. Using biogenic CO<sub>2</sub> to produce synthetic fuels offers a green alternative pathway to mitigate GHG emissions in the transportation and heating sectors, while decreasing reliance on fossil fuels. The displacement of each tonne of heavy fuel is estimated to prevent emissions of between 300 and 500 g of CO<sub>2</sub> eq.; this also applies to fossil fuel-derived chemicals.<sup>4</sup>

Biological methods of CO<sub>2</sub> conversion to renewable fuels and carbon based products, such as photosynthetic carbon assimilation by plants or algae, harness carbon dioxide using natural



Jerry D. Murphy

*Jerry Murphy serves as Director of the MaREI centre for energy, climate and marine. He has supervised to graduation c. 30 PhD researchers and has published c. 220 peer review journal papers. Scholar GPS ranks his work in the top 11 academics worldwide researching "Biofuels". He was awarded the Mary B Upton Visiting Professorship in Cornell University (fall 2024); and a visiting research fellow of The International*

*Energy Agency in Paris (2024). He serves as International Advisor to DBFZ (The German Bioenergy Research centre). Jerry has served as Professor Chair of Civil Engineering in University College Cork, Ireland since 2017.*





Fig. 1 Overview of microbial electro-synthesis pathways and derived bioproducts.

processes, but the whole lifecycle process from CO<sub>2</sub> to end product is inherently of low efficiency.<sup>5</sup> In contrast, non-biological catalysis provides precise process control and targeted CO<sub>2</sub> conversion without biological constraints, yet require high energy inputs (high pressure and temperature), selective catalysts, and may involve environmentally harmful chemicals such as toxic solvents, strong acids and bases. While both technologies have potential, each has limitations that must be addressed. A developing approach that has gained significant attention over the last decade is to combine electrochemical and biological processes to enhance the conversion of CO<sub>2</sub> into biomass and carbon-based goods; such processes are termed microbial electro-synthesis (MES)<sup>6,7</sup> as shown in Fig. 1. Microorganisms convert biogenic CO<sub>2</sub> into multicarbon products, powered by renewable electricity—typically supplied through an electrode. The valorisation of CO<sub>2</sub> to multicarbon compounds through MES is a one-step biosynthetic process under mild conditions, which offers simpler pathways than multi-step thermochemical processes.

The derived valuable chemical products include organic acids, alcohols, and bioplastics, with applications in the packaging, food, pharmaceutical, chemical, and renewable energy sectors. The conversion of CO<sub>2</sub> into these biochemical products presents a promising economic opportunity, despite currently exhibiting lower production rates.<sup>8,9</sup> At present, these compounds are predominantly synthesised through conventional thermal chemical processes relying on fossil-based feedstocks. The anticipated growth in their market demand, combined with increasing CO<sub>2</sub> emission-related costs, highlights the potential for MES to serve as a viable alternative technical pathway. For example, the global hexanoic acid market was valued at approximately €55 million in 2024 and is predicted to rise from €58 million in 2025 to nearly €93 million by 2034, representing a compound annual growth rate (CAGR) of 5.4% from the year 2025 to 2034.<sup>10</sup> A life cycle assessment by Luo *et al.*<sup>11</sup> assuming a nominal production capacity of 10 kt per year of purified hexanoic acid through MES assessed a carbon footprint of approximately 5.5 t CO<sub>2</sub> eq t<sup>-1</sup> hexanoic acid. This value is comparable to that of hexanoic acid derived from fermentation or plant-based pathways. When integrated with renewable energy, electrochemical CO<sub>2</sub> conversion technologies have the capacity to produce chemicals with a negative carbon

footprint.<sup>12</sup> Moreover, the decreasing cost of renewable electricity serves as an additional incentive for the development of MES at a cost-competitive rate.<sup>13,14</sup>

MES faces several technical challenges that hinder its scalability and industrial application, including the slow rate of CO<sub>2</sub> reduction, low product selectivity, high overpotential requirements and economic viability.<sup>15</sup> These limitations underscore the critical importance of electrode design, as it directly impacts the stability and scalability of the MES system. An electrode within a MES process ideally should be chemically stable, highly conductive, biocompatible and of low-cost.<sup>16</sup> While precious metal electrodes have shown improved performance, their high cost has increasingly directed attention towards more accessible and sustainable carbon-based materials for electrode production. Typically, the production of functional carbonaceous materials, such as graphene, activated carbon, and carbon nanotubes, relies on coal or petrochemical feedstocks. These methods often involve energy-intensive processes and harsh synthetic conditions, including high temperatures and complex operational procedures.<sup>17</sup> Therefore, developing efficient and sustainable methods for producing high-performance carbon materials with minimal environmental impact is urgently needed.

Biochar is a carbon-rich material produced through pyrolysis of dry organic materials or hydrothermal carbonisation of wet organic materials; it is characterised by high surface area, tunable porosity and versatile nanostructures.<sup>18</sup> When compared to fossil-fuel-derived activated carbon and carbon black, biochar production is recognised as a more sustainable process, as it enables the mitigation of anthropogenic CO<sub>2</sub> emissions through the conversion of biomass into a carbonaceous material. Traditionally biochar has been used as a soil amendment, in wastewater treatment, and for carbon sequestration. More recently biochar has been explored as a material with applications in energy storage and conversion, including use in lithium-ion and sodium-ion batteries, electrochemical sensors, supercapacitors, oxygen electrocatalysts, fuel cells and hydrogen energy systems.<sup>19</sup> Use in hydrogen energy systems includes for: physical adsorption of hydrogen; or as an additive in biological H<sub>2</sub> production; or as cathodic material in electrocatalytic H<sub>2</sub> evolution. According to Bolan *et al.*, biochar is much cheaper (712 € t<sup>-1</sup>) than commercially available activated carbon (1280 € t<sup>-1</sup>).<sup>20</sup> Building on its characteristics and economic feasibility, researchers are increasingly investigating the potential of biochar as an electrode material in MES to enhance system performance and accelerate the scalability of the process.

The application of waste-derived biochar electrodes in MES offers a promising avenue for advancing energy conversion efficiency, reducing investment costs, and fostering sustainable development. Current research predominantly emphasises the fundamental properties of biochar, while other aspects, such as its electrochemical performance and long-term stability within bio-electrochemical systems, remain insufficiently explored. Addressing these challenges is crucial for facilitating the transition of biochar-based MES systems from laboratory-scale studies to industrial-scale implementation. Therefore, through



focusing on MES as a leading energy conversion technology, this perspective aims to outline recent research advancements, highlighting the latest developments and challenges in MES applications equipped with biochar electrodes. This perspective will also explore how waste-derived biochar and MES reactor designs must evolve to enhance sustainability, improve integration with existing infrastructure, and support the transition to a circular economy.

## 2 Biochar: a renewable approach to environmental remediation and energy storage

### 2.1 Biomass as a sustainable resource for biochar production

In 2021, the global biomass supply in energy terms reached nearly 54 EJ,<sup>21</sup> highlighting its significance as a renewable and abundantly available resource. Biomass is primarily composed of cellulose, hemicellulose, and lignin, which readily decompose at temperatures below 700 °C.<sup>22</sup> This characteristic facilitates the pyrolysis of biomass at relatively low temperatures, leading to the production of biochar, bio-oil, and pyrolysis syngas (comprising of H<sub>2</sub>, CO, CO<sub>2</sub>, NO<sub>x</sub>, SO<sub>x</sub>, and H<sub>2</sub>S). Among these bioproducts, biochar, a carbon-rich material, has attracted attention due to its eco-friendly nature, and its potential for application in environmental remediation and energy storage.

Biochar is produced through thermochemical conversion techniques, primarily pyrolysis and hydrothermal carbonisation,<sup>23</sup> as shown in (Fig. 2). These processes involve the thermal decomposition of organic biomass at moderate temperatures (typically in the range 300–700 °C) in the absence of oxygen or with a limited oxygen supply.<sup>23</sup> The properties of

the biochar are heavily influenced by the pyrolysis process parameters (such as temperature, temperature ramp up rate, and holding time) and the type of feedstock used, including its composition, chemical structure, and cellulose or lignin content.<sup>24</sup> For example, woody biochar is characterised by its high carbon content (more than 70%) and porosity, which is particularly advantageous for carbon sequestration and soil water retention.<sup>25</sup> Biochar produced from the solid fraction of animal slurry is typically rich in nutrients (such as N, P, and K), making it effective for improving soil fertility and promoting nutrient cycling.<sup>26</sup>

Pyrolysis is a conventional thermal decomposition process in an oxygen-limited environment, where lignocellulosic biomass undergoes depolymerisation, cross-linking, and fragmentation for biochar (pyrochar) production.<sup>19</sup> This process typically requires dried biomass and operates with a pyrochar yield over 35% (see Table 1). Optimising production conditions such as heating rate, residence time, and temperature is crucial for achieving high-quality pyrochar. Hydrochar is a form of biochar produced through hydrothermal carbonisation, a process distinct from dry thermochemical methods such as pyrolysis. In hydrothermal carbonisation, biomass is mixed with water in a sealed reactor, where the temperature gradually increases. This process involves hydrolysis, followed by fragmentation, degradation and isomerization, which lead to the formation of intermediate products. These intermediates and derivatives then undergo condensation, polymerization, and intramolecular dehydration, resulting in hydrochar production.<sup>19</sup> The hydrothermal carbonisation process is better suited for nutrient-rich biochar production due to its retention of organic compounds. The process involves shorter residence times and the ability to process wet biomass without the need for prior drying, making it more energy-efficient than pyrolysis.



Fig. 2 The process of biochar production and some of its applications in environmental remediation and energy storage.





Table 1 The properties and applications of biochar derived from various biomass sources

| Biomass                                  | Synthesis method           | Operating conditions (temperature, inert gas and holding time)                     | Carbon content (%) | Surface area (m <sup>2</sup> g <sup>-1</sup> ) | Application scenario            | Performance  |
|--|----------------------------|--|--------------------|--|---------------------------------|--|
| Municipal sludge                         | Pyrolysis                  | 600 °C, N <sub>2</sub> , 2 h   | 32.7               | 19.2   | Pollutants removal              | Effectively remove >99.9% phosphate in anaerobic digestion liquid and wastewater <sup>33</sup> –BCO <sub>2</sub> and –OH were identified as the main active sites for peroxymonosulfate activation <sup>34</sup> |
| Sewage sludge                            | Pyrolysis                  | 600 °C, N <sub>2</sub> , 2 h   | 53.6               | 21.6   | Pollutants removal              | Efficient in adsorbing perfluoroalkyl and polyfluoroalkyl substances, cationic and anionic dyes, and pharmaceuticals and personal care products <sup>35</sup>  |
| Agrochemical and pharmaceutical sludge   | Pyrolysis                  | Phase 1: 800 °C, N <sub>2</sub> , 1 h;<br>Phase 2: 800 °C, N <sub>2</sub> , 30 min | 30.0               | 238.5  | Pollutants removal              | Simultaneous removal of As(III) and Cd(II) in aqueous solution by ferrhydrite-modified biochar <sup>36</sup>   |
| Rape straw                               | Pyrolysis                  | 400 °C, N <sub>2</sub> , 2 h   | NR <sup>a</sup>    | 3.8  | Pollutants removal              | The titanium-modified ultrasonic biochar achieved the maximum adsorption capacities of Cd(II) and As(V) at 72.6 and 118.1 mg g <sup>-1</sup> <sup>37</sup>   |
| Raw corncobs                             | Pyrolysis                  | 550 °C, N <sub>2</sub> , 2 h   | 81                 | 450.4  | Pollutants removal              | Adding 10 g L <sup>-1</sup> of biochar to two-stage digestion increased CH <sub>4</sub> yield by 24% <sup>25</sup>   |
| Commercial wood chips                    | Pyrolysis                  | 700 °C, NR, 1 h  | 87.8               | 161.5  | Anaerobic digestion improvement | Biochar increased CH <sub>4</sub> yield from willow digestion by 60% <sup>38</sup>   |
| Willow biomass ( <i>Salix purpurea</i> ) | Pyrolysis                  | 700 °C, N <sub>2</sub> , 1 h   | 57.9               | 4.1  | Anaerobic digestion improvement | Iron modified biochar increased CH <sub>4</sub> yield by 21.9% <sup>39</sup>   |
| Tea leaves                               | Pyrolysis                  | 600 °C, N <sub>2</sub> , 2 h   | 85.8               | 1.7  | Anaerobic digestion improvement | The biogas yield was improved to 1.4 L/L/d when adding 4.0% of corn straw biochar <sup>40</sup>  |
| Corn straw                               | Hydrothermal carbonisation | 600 °C, NR, 0.3 h  | 57.4               | 1.0  | Anaerobic digestion improvement | Biochar enriched dechlorinating bacteria and electroactive bacteria, thus enhanced electron transfer capacity <sup>41</sup>  |
| Sewage sludge                            | Pyrolysis                  | 800 °C, N <sub>2</sub> , 6 h   | 40                 | NR   | Anaerobic digestion improvement | The tomato ( <i>Solanum lycopersicum</i> ) seedlings increased by 13.1% over the stress controls by adding biochar <sup>42</sup>   |
| Fresh rice and corn stalks               | Pyrolysis                  | 350 °C, NR, 2 h  | 35                 | NR   | Soil amendment                  | Biochar restrained antibiotic resistance genes transmission from the soil and rhizosphere to endophytes <sup>43</sup>  |
| Rice husk                                | Pyrolysis                  | 500 °C, N <sub>2</sub> , NR  | 51.1               | 28.6   | Soil amendment                  | Biochar reduced content of four phthalates in radish roots and dibutyl phthalate in lettuce leaves <sup>44</sup>   |
| Pellets from sunflower                   | Pyrolysis                  | 600 °C, N <sub>2</sub> , 3 h   | 86.7               | 0.1  | Soil amendment                  | Biochar application improves soil pH, bacterial community structure and enzyme activity <sup>45</sup>  |
| Corn straw                               | Pyrolysis                  | 650 °C, N <sub>2</sub> , 2 h   | 93                 | 960  | Soil amendment                  | Olive stone biochar can substitute quarry aggregate in subgrade constructions <sup>46</sup>  |
| Olive stone                              | Pyrolysis                  | 600 °C, NR, NR   | 85.4               | NR   | Construction materials          | Biochar-modified concrete improved 28-day flexural strength by 18.9% due to microstructure modification and internal curing <sup>47</sup>  |
| Spent coffee grounds                     | Pyrolysis                  | 450 °C, NR, NR   | 67.5               | NR   | Construction materials          |  |



Table 1 (Contd.)

| Biomass                               | Synthesis method           | Operating conditions (temperature, inert gas and holding time)                          | Carbon content (%) | Surface area (m <sup>2</sup> g <sup>-1</sup> ) | Application scenario          | Performance  |
|---------------------------------------|----------------------------|---|--------------------|--|-------------------------------|--|
| Sewage sludge                         | Pyrolysis                  | 600 °C, N <sub>2</sub> , 2 h  | 40                 | 13.1   | Energy storage and conversion | Maximum power density at 9.1 mW m <sup>-2</sup> in a microbial fuel cell <sup>18</sup>   |
| <i>Camellia oleifera</i> shell powder | Hydrothermal carbonisation | Ultrasonic waves for 30 min.<br>Phase 1: 220 °C, NR, 24 h;<br>Phase 2: 180 °C, NR, 24 h | NR                 | 536.5  | Energy storage and conversion | Excellent reversible specific capacity (369.6 mA h g <sup>-1</sup> at a current density of 0.2 A g <sup>-1</sup> ) and significant initial coulombic efficiency (72.5%) in a microbial fuel cell <sup>49</sup> |
| Wood of <i>Acacia auriculiformis</i>  | Pyrolysis                  | 300 °C, NR, 1 h   | 80                 | 29   | Energy storage and conversion | High current density at 2.5 × 10 <sup>2</sup> mA m <sup>-2</sup> in a microbial fuel cell <sup>50</sup>  |
| Reeds                                 | Pyrolysis                  | 800 °C, N <sub>2</sub> , 2 h  | NR                 | NR   | Energy storage and conversion | 100% biochar electrodes, maximum output power density at 33.7 mW m <sup>-2</sup> in a microbial fuel cell <sup>51</sup>  |
| Corn stalks                           | Pyrolysis                  | 400 °C, NR, 10 h  | 84.0               | 3.1  | Energy storage and conversion | Maximum power density at 108.1 mW m <sup>-2</sup> in a microbial fuel cell <sup>52</sup>   |

<sup>a</sup> NR represents for not reported.

Additionally, hydrochar retains more oxygen-containing functional groups (such as hydroxyl and carboxyl) than pyrochar.<sup>27</sup> This increased functional group content improves its chemical reactivity and enhances its performance in ion exchange applications. However, hydrochar typically exhibits lower porosity than pyrochar, which may limit its use in applications that require a high surface area, such as material for energy storage or gas adsorption.

## 2.2 Biochar's composition and extensive surface area

Biochar primarily consists of carbon (C), hydrogen (H), oxygen (O), and other elements such as nitrogen (N), potassium (K), calcium (Ca), magnesium (Mg), and phosphorus (P). The C compounds include for fatty acids, phenols, and alcohols, while N is primarily found on the surface structure. The content of metals such as K, Ca and Mg varies depending on the source of the biochar, whether derived from animal slurry, agriculture residues or wood. Biochar is typically alkaline because of the presence of inorganic minerals such as carbonates and phosphates, thus can act as the soil amendment for raising soil pH. The pH of biochar generally increases with rising pyrolysis temperatures (up to 900 °C), primarily due to organic acid volatilisation and the breakdown of acidic functional groups such as carboxyl and phenolic hydroxyl. This alkalinity also helps maintain a favourable pH environment for electroactive microorganisms in the MES systems. The porosity and surface area of biochar are key attributes, typically ranging from 0.1 to 400 m<sup>2</sup> g<sup>-1</sup> depending on production conditions (see Table 1). Elevated pyrolysis temperatures typically enhance biochar porosity by promoting the volatilisation of tars and organic compounds that would otherwise fill the internal pores. However, this process also reduces the overall biochar yield due to mass loss.

The various functional groups on the surface of biochar, such as hydroxyl, carboxyl and carbonyl, are mostly oxygen-containing or alkaline. These functional groups enhance biochar's adsorption, ion exchange and buffering capacities due to their distinct chemical properties. The hydroxyl groups, for example, can facilitate the electron density of conjugated  $\pi$ -systems through their electron-donating property.<sup>28</sup> High-temperature pyrolysis enhances biochar's adsorption property by transforming less stable hydroxyl groups into more reactive carbonyl groups, improving their ability to interact with various water contaminants.<sup>29</sup> Additionally, biochar demonstrates remarkable stability due to its high level of carboxylate esterification, aromatisation, and resistance to biological, physical and chemical degradation. Its high carbon content (up to 93%) and inherent stability prove it to be a suitable material for long-term applications, for example, as an additive in cement to reduce its carbon footprint.<sup>30</sup> For MES, this stability ensures sustained electrochemical performance over extended operational cycles without any deterioration.

Biochar supplementation to anaerobic digestion has also been shown to enhance the digestion process by facilitating increased methane yields (up to 60%) and reduced lag-phase times (by 42%).<sup>25,31</sup> As a buffering agent, biochar has the

capacity to alleviate volatile fatty acid accumulation, and as such prevent inhibition of the anaerobic digestion process. The high surface area of biochar helps immobilise functional microorganisms, further supporting microbial activity during digestion. Some abundant oxygen-containing functional groups, such as quinone and hydroquinone, provide both electron-accepting and electron-donating capacities.<sup>32</sup> These functional groups facilitate the direct interspecies electron transfer process during anaerobic digestion, thus promoting efficient microbial activity for methane production. This redox activity is equally critical in MES, where biochar can function as a conductive electron transfer bridge between electroactive microbes and electrode surface.

### 2.3 Biochar's tunable porosity and surface functional groups

Biochar demonstrates significant potential as a versatile platform material for energy storage and conversion applications due to its tunable porosity and surface chemistry (Table 1). The porosity and surface functional groups of the electrode material play a significant role in determining reactor efficiency. The porous structure of biochar enhances the charge transfer kinetics at the electrode surface, while the surface functional groups, such as carboxyl and hydroxyl groups, influence the thermodynamics of heterogeneous reactions.<sup>19</sup> In MES systems, this synergistic effect between porosity and surface chemistry enables efficient mass transport of reactants. Bregadiolli *et al.* demonstrated that biochar synthesised from sugarcane bagasse exhibited higher specific capacitance than metal oxide composites, attributed to its larger surface area and higher medium pore diameter.<sup>53</sup> The porosity of biochar can be further optimised by water/acid washing or varied activations to improve its storage capacity in supercapacitors and batteries.<sup>54</sup> Furthermore, biochar-based nanostructured composites can be effectively designed by modifying the surface chemistry. These composites enhance conductivity and overall reactor efficiency by integrating the inherent properties of biochar with advanced materials. When applied to MES, such composites can improve electrode conductivity as well as minimise charge transfer resistance.

Typically, in hydrogen storage, biochar's microporous structure, enhanced through KOH, ZnCl<sub>2</sub> or steam activation, facilitates hydrogen adsorption *via* capillary forces.<sup>55,56</sup> The surface functional groups, such as alkali metals, further improves hydrogen storage performance by chemisorption. For example, potassium and sodium species in biochar act as alkaline cores, attracting and stabilising hydrogen molecules.<sup>56</sup> In biological hydrogen production *via* dark fermentation, biochar enhances the interspecies electron transfer efficiency by utilising its redox-active functional groups, such as quinone and hydroquinone.<sup>25</sup> Biochar also supports bacterial growth and stabilises dark fermentation due to its pH buffering capacity, reducing the lag phase in hydrogen production.<sup>25</sup> In the electrocatalytic hydrogen evolution reaction *via* water splitting, biochar integrated with catalytically active species serves as an effective electrocatalyst, reducing overpotential and increasing current densities.<sup>57</sup> Heteroatom doping and single atom doping in biochar have demonstrated potential to

enhance the number of active catalytic sites,<sup>58,59</sup> though further research is needed to fully understand the catalytic mechanisms and optimise performance. With ongoing advancements in biochar-based nanostructured composites, it may be said that biochar holds great promise as a cost-effective alternative to expensive materials in energy and MES systems.

## 3 Microbial electrosynthesis: a bioelectrochemical approach to CO<sub>2</sub> utilisation and conversion

### 3.1 The integration of electrocatalysis with biocatalysis

Microbial electrosynthesis or MES is an advanced bioelectrochemical technology that employs microorganisms as biocatalysts to facilitate the reduction of CO<sub>2</sub> into value-added organic compounds using electrons supplied by a cathode. Electrocatalysis enables the efficient conversion of CO<sub>2</sub> into simple intermediates such as carbon monoxide (CO) and formic acid (CH<sub>2</sub>O<sub>2</sub>), while biocatalysis facilitates carbon-carbon bond coupling for the synthesis of commercially valuable compounds such as glucose (C<sub>6</sub>H<sub>12</sub>O<sub>6</sub>), fatty acids and alcohols.<sup>7,60</sup> By integrating electrocatalytic and biocatalytic processes, MES offers an efficient strategy to overcome energy constraints and enhance the selective production of long-chain organic molecules from CO<sub>2</sub>.

In a typical MES, chemolithoautotrophic microbes facilitate CO<sub>2</sub> reduction at the cathode through two primary electron transfer mechanisms: direct electron transfer or mediated electron transfer *via* H<sub>2</sub> or other soluble redox mediators.<sup>61</sup> In direct electron transfer, microorganisms obtain electrons directly from the electrode *via* conductive bacterial pili or membrane-bound cytochromes. For example, *Sporomusa ovata* has been shown to accept cathodic electrons directly to synthesise multi-carbon compounds from CO<sub>2</sub> and water.<sup>62</sup> Other microbes, such as *Geobacter* and *Clostridium* species, use conductive pili or c-type cytochromes to conduct electron transfer at the abiotic-biotic interface.<sup>63</sup> In contrast, mediated electron transfer relies on soluble redox mediators to facilitate electron transfer between the electrode and microbial metabolism. For example, H<sub>2</sub> generated through water electrolysis can act as an intermediary, enabling microorganisms to assimilate CO<sub>2</sub> through metabolic pathways such as the Wood-Ljungdahl pathway.<sup>64</sup>

As compared to pure abiotic electrochemical CO<sub>2</sub> reduction, MES enables the selective synthesis of long-chain organic products that are challenging to obtain through traditional chemical catalysis.<sup>61</sup> Microbial catalysts exhibit robust operational stability and self-replicating capabilities, reducing costs associated with catalyst degradation and replacement. MES operates efficiently across a wide range of environmental conditions, including varying pH, temperatures, and pressures, making it adaptable to diverse applications.<sup>12</sup>

### 3.2 Products generated from MES in power-to-gas and power-to-fuel applications

Biogas produced through anaerobic digestion typically contains 30–50% CO<sub>2</sub>, which requires removal before the CH<sub>4</sub> can be used in industrial applications. MES can be applied as an *in situ*



Table 2 Multiple bioproducts generated from microbial electrosynthesis using various cathode materials<sup>a</sup>

| Bioelectrochemical reaction   | Products       | Cathode material  | Scale               | The function of biochar  | Performance  |
|---|----------------|---|---------------------|--|--|
| $\text{CO}_2 + 8\text{H}^+ + 8\text{e}^- \rightarrow \text{CH}_4 + 2\text{H}_2\text{O}$                           | Methane        | Dual Pt/C carbon cloth and carbon nanoparticle-coated stainless-steel mesh layers | Lab scale; 5 mL     | NA   | The $\text{CH}_4$ production rate was $16 \text{ L L}^{-1}$ per day at $54 \text{ A m}^{-2}$ , with an applied voltage of $2.8 \text{ V}$ . It reached a maximum energy efficiency of 34%, among the highest methane production rates in microbial electrosynthesis. <sup>73</sup> |
| $\text{CO}_2 + 8\text{H}^+ + 8\text{e}^- \rightarrow \text{CH}_4 + 2\text{H}_2\text{O}$                           | Methane        | Stainless steel woven mesh  | Pilot scale; 20 L   | NA   | The reactor achieved an average methane production rate of $0.53 \text{ L L}^{-1}$ per day, with a peak rate of $0.68 \text{ L L}^{-1}$ per day, while maintaining a high average coulombic efficiency of 98%. <sup>74</sup>   |
| $\text{CO}_2 + 8\text{H}^+ + 8\text{e}^- \rightarrow \text{CH}_4 + 2\text{H}_2\text{O}$                           | Methane        | Biochar coated carbon cloth   | Lab scale; 28 mL    | Wood chips (WC)/Organic municipal solid waste (OW) biochar cathode       | The $\text{CH}_4$ production with WC-biochar cathode achieved $3.6 \text{ mL day}^{-1}$ at 73% v/v, while with OW-biochar cathode achieved $3.0 \text{ mL day}^{-1}$ at 70% v/v. <sup>75</sup>   |
| $2\text{CO}_2 + 8\text{H}^+ + 8\text{e}^- \rightarrow \text{CH}_3\text{COOH} + 2\text{H}_2\text{O}$               | Acetic acid    | Biochar coated carbon cloth   | Lab scale; 120 mL   | WC/OW derived biochar as cathode   | The acetate production with WC-biochar cathode achieved $0.3 \text{ g L}^{-1} \text{ day}^{-1}$ , while with OW-biochar cathode achieved $0.03 \text{ g L}^{-1}$ per day. <sup>75</sup>  |
| $2\text{CO}_2 + 8\text{H}^+ + 8\text{e}^- \rightarrow \text{CH}_3\text{COOH} + 2\text{H}_2\text{O}$               | Acetic acid    | Carbon felt   | Pilot scale; 12.6 L | NA   | The pilot-scale microbial electrosynthesis system produced acetic acid at a rate of $71 \text{ g m}^{-2}$ per d with a coulombic efficiency of 77.8%. <sup>76</sup>  |
| $2\text{CO}_2 + 8\text{H}^+ + 8\text{e}^- \rightarrow \text{CH}_3\text{COOH} + 2\text{H}_2\text{O}$               | Acetic acid    | Hydrochar coated carbon felt  | Lab scale; 250 mL   | Sludge-derived hydrochar as a cathode catalyst                           | The application of hydrochar composite catalysed cathode in MES nearly doubled acetate production, reaching $2.4 \text{ g L}^{-1}$ as compared to the uncatalysed system. <sup>77</sup>  |
| $3\text{CO}_2 + 14\text{H}^+ + 14\text{e}^- \rightarrow \text{CH}_3\text{CH}_2\text{COOH} + 4\text{H}_2\text{O}$  | Propionic acid | Carbon felt   | Lab scale; 400 mL   | NA   | A production rate of $0.35 \text{ g L}^{-1}$ per day for propionic acid was achieved under an applied cathode potential of $-0.8 \text{ V}$ . <sup>78</sup>  |
| $4\text{CO}_2 + 20\text{H}^+ + 20\text{e}^- \rightarrow \text{C}_4\text{H}_8\text{O}_2 + 6\text{H}_2\text{O}$     | Butyric acid   | Carbon felt   | Lab scale; 200 mL   | NA   | A maximum butyric acid concentration of $0.7 \text{ g L}^{-1}$ was achieved using a nano zero-valent iron dosage of $7.5 \text{ g L}^{-1}$ (ref. 79)   |
| $4\text{CO}_2 + 20\text{H}^+ + 20\text{e}^- \rightarrow \text{C}_4\text{H}_8\text{O}_2 + 6\text{H}_2\text{O}$     | Butyric acid   | MXene-biochar packed stainless steel mesh   | Lab scale; 200 mL   | MXene coated biochar (derived from rice straw pyrolysis) as a biocathode | Butyric acid production with MXene-coated biochar cathode achieved $1.1 \text{ g L}^{-1}$ , which is 1.7 times higher than the uncoated cathode. <sup>80</sup>   |
| $6\text{CO}_2 + 36\text{H}^+ + 36\text{e}^- \rightarrow \text{C}_6\text{H}_{12}\text{O}_2 + 12\text{H}_2\text{O}$ | Hexanoic acid  | Carbon felt   | Lab scale; 250 mL   | NA   | The highest hexanoic acid concentration reached $8.0 \text{ g L}^{-1}$ , with a selectivity of 47% among the volatile fatty acids under $-1.0 \text{ V}/\text{CO}_2$ condition. <sup>81</sup>  |
| $\text{CO}_2 + 6\text{H}^+ + 6\text{e}^- \rightarrow \text{CH}_3\text{OH} + \text{H}_2\text{O}$                   | Methanol       | Cofactor NADH, metal organic framework ZIF-8/Rh complex-grafted electrode         | Lab scale; 25 mL    | NA   | A methanol concentration of $23.7 \text{ mg L}^{-1}$ was achieved at a production rate of $822 \text{ } \mu\text{mol g}^{-1} \text{ h}^{-1}$ (ref. 82)   |
| $2\text{CO}_2 + 12\text{H}^+ + 12\text{e}^- \rightarrow \text{C}_2\text{H}_5\text{OH} + 3\text{H}_2\text{O}$      | Ethanol        | 3D cobalt-nickel-coated carbon felt   | Lab scale; 250 mL   | NA   | The maximum ethanol concentration achieved was $0.2 \text{ g L}^{-1}$ at an applied voltage of $3.0 \text{ V}$ . <sup>83</sup>   |



Table 2 (Contd.)

| Bioelectrochemical reaction   | Products                  | Cathode material     | Scale             | The function of biochar | Performance  |
|---|---------------------------|----------------------|-------------------|-------------------------|--|
| $4\text{CO}_2 + 24\text{H}^+ + 24\text{e}^- \rightarrow \text{C}_4\text{H}_9\text{OH} + 7\text{H}_2\text{O}$  | Butanol                   | Titanium mesh        | Lab scale; 250 mL | NA                      | The highest butanol concentration achieved was $0.4 \text{ g L}^{-1}$ at a cathode potential of $-0.9 \text{ V}$ (vs. Ag/AgCl) <sup>84</sup>   |
| $2\text{CO}_2 + 8\text{H}^+ + 8\text{e}^- \rightarrow \text{CH}_3\text{COOH} + 2\text{H}_2\text{O}$ ;<br>acetate + $\text{O}_2 \rightarrow$ single cell protein | Single cell protein       | Stainless steel mesh | Lab scale; 6 L    | NA                      | A microbial electrosynthesis cell was connected to a single-cell protein fermenter. The obtained cell dry weight was $32.8 \text{ g L}^{-1}$ at a production rate of $1.14 \text{ g L}^{-1}$ per day. The biomass contained a protein content of up to 73% <sup>85</sup> |
| $\text{CO}_2 \rightarrow$ volatile fatty acids $\rightarrow$ bioplastics  | Polyhydroxybutyrate (PHB) | Graphite plate       | Lab scale; 1 L    | NA                      | PHB accumulation reached $2.44 \text{ mg/gVSS}$ in single step microbial electrosynthesis cells under an optimal applied voltage of $2.5 \text{ V}$ <sup>86</sup>  |
| Acetate $\rightarrow$ acetyl-CoA $\rightarrow$ fatty acyl-CoA $\rightarrow$ fatty alcohols  | Lipids                    | Graphite plate       | Lab scale; 150 mL | NA                      | Fatty alcohol production by the engineered strain <i>Yarrowia lipolytica</i> YLFL-11 reached $83.8 \text{ mg g}^{-1}$ dry cell weight <sup>87</sup>  |

<sup>a</sup> NA represents not applicable.

biogas upgrading method by integrating electrodes into anaerobic digesters. This biomethanation process, a power-to-gas approach, enables the biological conversion of  $\text{CO}_2$  into  $\text{CH}_4$  through microbial metabolic processes (eqn (1)–(3)) as shown in Table 2. In such electrode-assisted anaerobic digestion systems, several key microbial communities are enriched to facilitate the fermentation process. Hydrolytic bacteria are enriched to break down recalcitrant organic compounds, promoting hydrolysis and increasing methane yield. Acetogens, such as *Syntrophomonas* and *Syntrophobacter*, can be enriched to convert fatty acids such as propionic acid ( $\text{C}_3\text{H}_6\text{O}_2$ ) and butyric acid ( $\text{C}_4\text{H}_8\text{O}_2$ ) into acetic acid ( $\text{C}_2\text{H}_4\text{O}_2$ ), which is then utilised by the acetogenic methanogens for methanogenesis.<sup>65</sup> Exoelectrogens, including *Stenotrophomonas* and *Geobacter*, are enriched to facilitate electron transfer at the electrode interface, facilitating the overall energy conversion efficiency.<sup>66</sup> These microbes work synergistically to enhance the efficiency of the electrode-driving biomethanation process. Ning *et al.* demonstrated that the use of electrochemical-acid pre-treated graphite cathodes in anaerobic digestion systems significantly enhanced biomethane production from grass silage and cattle slurry, resulting in a 96.8% increase in yield, and a 32.5% increase in  $\text{CH}_4$  concentration in the output biogas.<sup>67</sup> The energy return from the increased biomethane output was 6.5 times higher than the additional electrical energy input, highlighting the catalytic role of electrical energy.<sup>67</sup>



MES also plays a crucial role in power-to-fuel applications, such as the production of liquid biofuels including alcohols and  $\text{C}_2$ – $\text{C}_6$  carboxylic acids<sup>68</sup> (Fig. 1). Acetate remains the most common and feasible end-product as shown in Table 2, as its production through the Wood–Ljungdahl pathway is the most energy-efficient carbon fixation mechanism, avoiding other ATP-consuming reactions by coupling endergonic and non-ATP-consuming exergonic reactions (eqn (4)–(7)). Cui *et al.* developed an electrolytic bubble column for  $\text{CO}_2$ -to-acetate production, achieving an acetate yield of up to  $34.5 \text{ g L}^{-1}$  and a production rate of  $1.15 \text{ g (L per day)}$ , with a faradaic efficiency of 64%.<sup>69</sup> Wild-type acetogens are capable of producing ethanol ( $\text{C}_2\text{H}_6\text{O}$ ), a widely used biofuel. In co-culture systems, various microbial species can further convert ethanol into highly energy-dense compounds, such as *n*-butanol ( $\text{C}_4\text{H}_{10}\text{O}$ ), *n*-hexanol ( $\text{C}_6\text{H}_{14}\text{O}$ ) and caproic acid ( $\text{C}_6\text{H}_{12}\text{O}_2$ ) through chain elongation.<sup>70</sup> As the worldwide carboxylic acid market is growing due to the huge demand for cosmeceutical products, butanol and hexanol can be directly integrated into the existing fuel infrastructure. Ning *et al.* demonstrated a faradaic efficiency of



up to 90.8% for the co-production of acetate and ethanol using a 3D cobalt-nickel-coated carbon felt biocathode in a MES system.<sup>71</sup> Liew *et al.* reported production rates of iso-propanol (C<sub>3</sub>H<sub>8</sub>O) and acetone (C<sub>3</sub>H<sub>6</sub>O) at approximately 3 g (L per h) with a selectivity up to 90% at a pilot scale MES system.<sup>72</sup> By integrating the MES with mixed microbial cultures, genetically engineered yeasts can also convert acetate into lipids or alkanes.<sup>61</sup> The commercial viability of MES-based fuels, however, depends on the development of efficient extraction and separation techniques, since most liquid biofuels require energy-intensive purification methods such as distillation, pervaporation, or solvent extraction.



### 3.3 Optimisation of cathode materials: advancing electron transfer and microbial attachment

One of the primary challenges in MES lies in optimising cathode materials to enhance electron transfer efficiency and microbial attachment. Various metals, including iron (Fe), nickel (Ni), copper (Cu), platinum (Pt) and gold (Au), have been investigated as cathode materials due to their high conductivity. However, these metallic cathodes often suffer from poor long-term stability due to metal leaching, which can inhibit microbial growth. As a result, carbon-based materials are still the most widely used cathodes for CO<sub>2</sub> bioconversion in MES.<sup>88</sup>

Graphite is available as a commercial electrode in the form of plates, rods, sticks, and granules. While widely adopted, pure graphite plates or rods have limitations in achieving high productivity due to their low porosity and limited surface area for microbe attachment. It is also considered a critical raw material in the EU due to potential supply chain challenges. To address this, 2D carbonaceous materials, such as carbon cloth, have gained attention due to their flexibility and higher porosity compared to traditional graphite electrodes. A porous ceramic hollow tube wrapped with carbon cloth was used by Alqahtani *et al.* as the cathode for direct CO<sub>2</sub> delivery to CO<sub>2</sub>-fixing microbial communities growing on the surface.<sup>89</sup> Beyond 2D materials, 3D carbon-based electrodes such as carbon foam, carbon felt, and brushes have also been explored for MES applications. With a larger volume reactive surface area, the 3D structure of these electrodes supports spatial modifications and facilitates efficient electron transport through catalytic reactive sites *via* direct or mediated transfer processes. Cheng *et al.* investigated a carbon felt-based cathode in MES and demonstrated that an iron-doped zeolite imidazolate framework-67 acted as an electron shuttle, enhancing CO<sub>2</sub> conversion to CH<sub>4</sub> 1.6-fold by promoting the expression of heme protein-

related genes and accelerating indirect electron transfer through cytochrome C.<sup>90</sup>

Researchers have investigated advanced cathode designs incorporating nanomaterials, coatings, and dedicated electrode architectures.<sup>91</sup> Improved surface chemistry can positively impact bacterial attachment through electroactive nano-surfaces, leveraging hydrogen bonding, electrostatic attraction, and van der Waals interactions. For example, metal-organic framework (MOF) coatings on carbon felt have been used to create super hydrophilic interfaces that support biofilm formation. Xia *et al.* introduced the MOF-derived hierarchical nanoarrays for use as biocathodes in MES, optimising electric field intensity and incorporating a heterojunction to enhance electron transfer.<sup>64</sup> The approach achieved a 9.6-fold increase in CH<sub>4</sub> production and a maximum current density of 10 A m<sup>-2</sup> as compared to the control.<sup>64</sup> Kracke *et al.* demonstrated efficient electro-methanogenesis using NiMo-graphite cathodes.<sup>92</sup> With a pure culture of *Methanococcus maripaludis*, the system achieved a high volumetric CH<sub>4</sub> production rate of 2.2 L<sub>CH<sub>4</sub></sub> per L<sub>reactor</sub> per day and close to 100% utilisation of the *in situ* evolved hydrogen at the cathode.<sup>92</sup> Advancements in 3D printing technologies have enabled the fabrication of customisable electrodes with specific geometric structures and channel sizes, offering new possibilities for the MES cathode design.<sup>93</sup> It was demonstrated that the 3D printed rGO/Fe<sup>3+</sup>/Fe<sub>3</sub>O<sub>4</sub> aerogel bioelectrode achieved a volumetric current density of 10 608 A m<sup>-3</sup>, the highest observed with pure *Geobacter sulfurreducens*.<sup>94</sup> This was due to the hierarchical pores of the rGO aerogel, which improved substrate mass transfer and bacterial attachment, along with magnetite nanoparticles that potentially enhanced interfacial electron transfer.<sup>94</sup>

## 4 The utilisation of waste-derived biochar in microbial electrosynthesis

### 4.1 Can biochar be engineered as an efficient cathode material in MES?

Biochar, derived from biomass pyrolysis, is a promising material for MES cathodes due to its distinctive physicochemical properties. It retains the intrinsic electrical conductivity and structural stability of carbon-based materials while also offering high porosity and biocompatibility, which enhances microbial attachment and electron transfer in MES system. Thulluru *et al.* investigated the use of sludge-derived hydrochar as an effective cathode catalyst in MES systems, demonstrating its ability to enhance electrochemical performance and CO<sub>2</sub> conversion. This improvement is attributed to its high specific surface area, abundant functional groups, and pyridinic and graphitic nitrogen. Their study achieved an acetate production of 41.14 ± 5.03 mmol L<sup>-1</sup>, a faradaic efficiency of 52% and a carbon recovery efficiency of 45%.<sup>77</sup> Wood chip derived biochar demonstrated better performance as a cathode material in MES systems, achieving higher CH<sub>4</sub> concentration at 73.2% and ten times greater acetic acid production (0.3 g L per day) compared to municipal solid waste-based biochar.<sup>75</sup> This enhanced efficiency in CH<sub>4</sub> or acetate production is attributed to higher



surface area and carbonaceous graphite-like structure, which improved electrochemical activity.

As pristine biochar often lacks the consistency and high conductivity required for MES applications, it needs to be engineered or modified to enhance its electrochemical properties for effective use. Biochar can function as an effective carrier for active components and can be tailored to improve cathode performance. By introducing functional groups (such as transition metal-based materials, hydroxides and sulfides) onto the biochar surface,<sup>64</sup> proton absorption can be facilitated, promoting electron shuttling and subsequent CO<sub>2</sub> reduction. Additionally, the incorporation of nanowires or nanoparticles increases the pore-specific surface area, providing active attachment sites for microbial communities, thereby enhancing biofilm formation.<sup>57</sup> Furthermore, biochar's adaptability allows for easy customisation and 3D printing into specialised chemical structures, enabling precise control over its properties for specific application scenarios. For example, in a designed MES system, the incorporation of multilayered conductive MXene onto a rice straw-derived biochar electrode significantly enhanced active sites, facilitated mass transfer, and promoted microbial growth, leading to a 2.3-fold increase in current density and a 1.7-fold enhancement in butyrate production compared to the uncoated control.<sup>80</sup> The integration of an iron-carbon micro-electrolysis matrix with a coconut shell biochar compound substrate enhanced CO<sub>2</sub> electrosynthesis, improving organic carbon removal efficiency to 93.5% by promoting the production of extracellular polymeric substances, volatile fatty acids, polyhydroxyalkanoate, and glycogen in cathode reactors.<sup>95</sup>

The cost evaluation of biochar-based electrode indicates that it provides a more sustainable and economically viable alternative to traditional carbon-based electrode materials, such as graphite and activated carbon. According to the market report 2024 by the European Biochar Industry Consortium, biochar production capacity in Europe has demonstrated substantial expansion. In 2023, the total amount of biochar production reached 75 000 tonnes, with an anticipated sustained growth rate of 55% from 2023 to 2024.<sup>96</sup> By the end of 2023, almost 70% of the production capacity was distributed in three dominant countries; Denmark, Finland, and Sweden. Huggins *et al.* investigated the use of biochar derived from forestry residues and compressed milling residues as electrode material in microbial fuel cells.<sup>97</sup> The study pointed out that the biochar electrode led to significantly reduced costs, with a material price ranging from 54–401 € t<sup>-1</sup>, which is lower than that of granular activated carbon (843–2635 € t<sup>-1</sup>) or graphite granules (527–843 € t<sup>-1</sup>).<sup>97</sup> Another techno-economic analysis demonstrated the feasibility of using lignin-derived porous biochar from yellow pine and switchgrass as electrode material for high-energy-density supercapacitors. As a tailored supercapacitor-grade biochar, yellow pine and switchgrass biochar can be produced at a minimum selling price of 9033 and 7094 € t<sup>-1</sup>, respectively, which are comparable to those of commercially available supercapacitor-grade activated carbon.<sup>98</sup>

The properties of biochar electrodes vary depending on the feedstock source and manufacturing process, with their key

advantages primarily associated with economic and environmental benefits rather than electrochemical performance. A previous study highlighted the feasibility and sustainability of biochar-derived activated carbon produced from *Prosopis juliflora* for supercapacitor applications. According to Sivaraman *et al.*, biochar-based activated carbon demonstrated 28% lower global warming potential than coal-based activated carbon.<sup>99</sup> This relatively slight difference may be attributed to the high pyrolysis (750 °C) and activation temperatures required for biochar production, which contribute to increased energy consumption.<sup>99</sup> To enhance the sustainability of biochar production, further research is required to optimise the process, such as utilising renewable electricity, optimising process parameters, exploring alternative activation methods, and sourcing sustainable raw biomaterials.

#### 4.2 Current challenges and opportunities for scaling up the MES technology

Currently, the MES technology remains at the proof-of-concept stage and requires extensive research to overcome scaling challenges before it can be considered for practical applications. The scale-up of MES technology is mainly constrained by factors such as limited current density, practical and long-term viability, material costs and integration with existing infrastructure.<sup>100,101</sup> The largest MES scale-up experiments with pure culture bioelectro-methanogenesis have reached a capacity of 50 L, achieving a methane production rate of 0.27 L per day (11.7 mmol per day).<sup>102</sup> Scaling up resulted in lower current densities compared to lab-scale systems, primarily due to high internal resistance in larger electrodes, which hindered methane production. To enhance performance at larger scales, it is essential to establish key scale-up criteria that maintain system efficiency. The scale-up processes of microbial fuel cells can provide valuable insights for the industrialisation of MES, as they share similar fundamental principles. For example, a scaled-up microbial fuel cell of 1000 L, consisting of 50 modules, was operated successfully for one year to treat municipal wastewater, achieving a COD removal rate of 70–90%.<sup>103</sup> The investment for the system was comparable to other scaled-up reactors per unit volume, with cost analysis indicating potential reductions using cheaper or alternative raw materials.

The economic analysis by Christodoulou *et al.* revealed that among five alternative compounds (formic acid, acetic acid, propionic acid, methanol and ethanol) produced from the MES, formic acid (CH<sub>2</sub>O<sub>2</sub>) and ethanol (C<sub>2</sub>H<sub>6</sub>O), with production costs of 0.36 € kg<sup>-1</sup> and 1.06 € kg<sup>-1</sup> respectively, are cost competitive, despite their long pay-back period of 15 years for a 1000 t per year production plant.<sup>104</sup> Both products were found to offer higher Internal Rates of Returns, with formic acid at 21% and ethanol at 14%, respectively, exceeding the industry's required rates of returns of 11.60%. This suggests that currently formic acid and ethanol production could enhance the viability and compatibility of the MES process. A dynamic simulation by Shemfe *et al.* assessed formic acid synthesis in a MES system for wastewater treatment.<sup>105</sup> The simulation assumed COD removal *via* anodic oxidation and CO<sub>2</sub> conversion to formic acid through



cathodic reduction. Life cycle analysis indicated the net savings of 4.3 kg CO<sub>2</sub> eq. in climate change impact and 61 MJ in resource consumption per kilogram of formic acid production.<sup>105</sup> The modular design of MES systems allows for cost-effective scaling by replicating an optimised and proven module to achieve the required throughput. These developments provide a technological roadmap for MES adoption, emphasising the need for continued research and investment in process scalability.

### 4.3 Integration of microbial electrosynthesis with biomethane facilities

The technology readiness levels (TRLs) for the MES technology alone currently ranges from 3 to 4, while the integration of bioelectrochemical technology in hybrid systems could further accelerate the progress to TRLs 6 or 7 in an industrial environment. Among the most promising approaches for MES scale-up is the cascading electrochemical biorefinery system combined with biomethane facilities (see Fig. 3). Demonstration plants incorporating water electrolysis before fermentation have successfully stored methane within the natural gas infrastructure, validating the feasibility of power-to-gas with biomethanation applications.<sup>106</sup> Scale-up strategies such as mixed bubble columns have reached high methane production rates while reducing energy consumption, demonstrating a viable pathway for MES integration.<sup>107</sup> A previous economic viability study assessed the feasibility of converting CO<sub>2</sub> to CH<sub>4</sub> in a MES system integrated within a biogas facility producing 345 Nm<sup>3</sup> of biomethane per day.<sup>108</sup> The results indicated that the MES system could increase total biomethane yield from biogas by 17.5% while reducing CO<sub>2</sub> emissions from the biogas upgrading process by 42.8%, with a techno-economic assessment identifying electricity demand as the primary cost driver.<sup>108</sup>

Anaerobic digestion is integral to a circular economy approach, transforming organic waste into renewable energy vectors (biomethane), biogenic CO<sub>2</sub>, and organic biofertilisers (digestate). One tonne of biomethane generates approximately two tonnes of biogenic CO<sub>2</sub>. In 2020, Europe had the capacity to produce an estimated 24 million tonnes of biogenic CO<sub>2</sub>, based on the biogas and biomethane volumes generated that year (18 billion cubic meters). CO<sub>2</sub> capture technologies are well-developed and have been integrated into 1000 biomethane facilities (at scales of 50 to 2000 Nm<sup>3</sup> h<sup>-1</sup>) across Europe as of 2021.<sup>109</sup> The number of biomethane plants in Europe increased from 1548 to 1678 between the 2024 and 2025 data collection periods, as reported in the latest European Biomethane Map 2025.<sup>110</sup> Germany still represents the highest level of biogenic CO<sub>2</sub> production among the EU Member States. By 2030, it is estimated that the EU could generate up to 46 million tonnes of biogenic CO<sub>2</sub>, with an anticipated production of 35 billion cubic meters of biomethane as outlined in the RePowerEU Plan.<sup>111</sup> It is estimated that the typical quantity of CO<sub>2</sub> captured from biogas facilities is 4000 to 50 000 tonnes CO<sub>2</sub> plant per year. During the anaerobic digestion process, capturing CO<sub>2</sub> comes at a relatively low cost (approximately 30 € t<sup>-1</sup>) due to its high CO<sub>2</sub> purity as compared to biomass combustion (costing 100 € t<sup>-1</sup>) and direct air capture (400 € t<sup>-1</sup>). With abundant biogenic CO<sub>2</sub> supply and well-developed CO<sub>2</sub> capture technologies, when integrated into existing biogas infrastructure, MES has the potential to displace fossil-based products with biogenic CO<sub>2</sub>-derived chemicals and fuels, contributing to net-zero carbon emissions (Fig. 3).

As concluded in this perspective, biochar is a promising electrode material for the MES process. When integrating MES with biomethane facilities, solid digestate from anaerobic digestion can be pyrolyzed or hydrothermally carbonised to produce biochar (pyrochar or hydrochar) for electrode

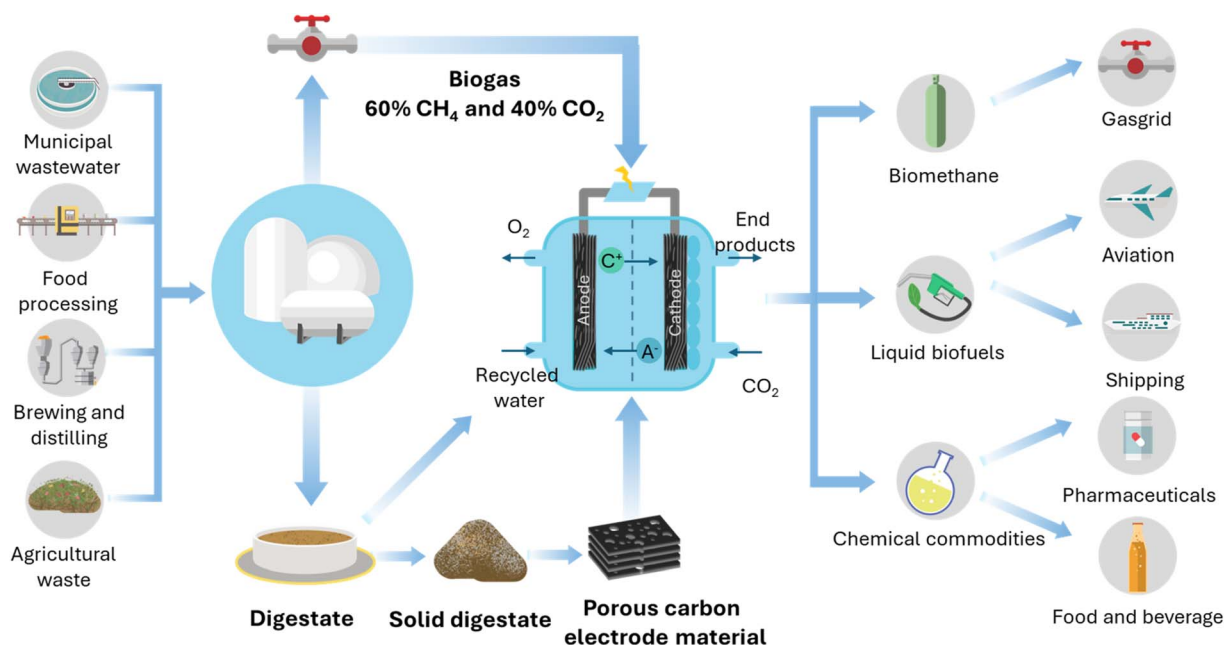


Fig. 3 Integration of microbial electrosynthesis with biomethane facilities within circular economy systems.



production. Recycled water from the digestion process can be employed as an electrolyte in the electrochemical biorefinery system, further reducing resource consumption. This recycled system not only enhances carbon recovery but also ensures sustainable utilisation of organic waste. Furthermore, integrating MES with biomethane facilities addresses the high electricity cost challenge by utilising on-site biomethane-generated electricity or surplus renewable energy,<sup>12</sup> reducing dependence on the power grid. This synergy creates a closed-loop system that enhances overall sustainability and contributes to global carbon mitigation efforts.

## 5 Future perspectives

Biochar, derived from abundant biomass sources, presents a promising and sustainable solution for both environmental remediation and energy storage. The diverse properties of biochar, such as high porosity, surface area, and functional groups, makes it effective in soil enhancement, pollutant adsorption, and improving anaerobic digestion processes. Biochar's versatility extends to energy storage, where its tunable properties facilitate its use in supercapacitors, batteries, and hydrogen storage systems, offering potential for cost-effective and efficient energy solutions. Furthermore, the ability of biochar to be tailored for specific applications, including as a catalyst or electrode material, opens new avenues for innovation in energy conversion and storage technologies. However, further research is needed to optimise consistent production processes and better understand of long-term effects in industrial applications.

Microbial electrosynthesis (MES) is a promising bioelectrochemical technology for CO<sub>2</sub> conversion, offering an innovative approach to produce value-added organic compounds whilst addressing environmental challenges. By integrating electrocatalysis with biocatalysis, the MES system enables the efficient reduction of CO<sub>2</sub> into simple intermediates and complex organic molecules, such as alcohols, fatty acids, and alkanes, with the potential for industrial applications by modular design in power-to-gas and power-to-fuel processes. The synergistic action of microorganisms and electrochemical systems allows for the selective production of long-chain products that are difficult to achieve through traditional chemical methods.

One of the key challenges of MES advancement is cathode optimisation, as it plays a vital role in enhancing electron transfer and microbial attachment. The development of advanced cathodes, such as 3D carbon-based electrodes and nanomaterial coating, has shown significant improvements in efficiency and stability, enabling better performance in MES systems. Biochar electrodes offer economic advantages, being more cost-effective than traditional carbon-based electrodes. Tailoring biochar with functional groups and incorporating nanoparticles or nanowires further enhances its performance. However, further research is needed to optimise the consistent production of biochar from different waste biomass and evaluate its full lifecycle advantages.

The scale up of MES technologies faces challenges including for limited current density, high material costs, the need for refined techno-economic models and life cycle analyses and difficulties in integration with existing infrastructure. Current systems are still at the proof-of-concept stage, but progress is being made with demonstration trials at 50 L scale, and a focus on high-value products, such as formic acid or ethanol. A few case studies show the potential for MES integration into existing industrial processes, especially when combined with biogas facilities. Biochar derived from biowastes may have the potential to be used as an efficient cathode material, while water can be recycled as the electrolyte, reducing resource consumption and enhancing carbon recovery. The coupling of MES with biomethane facilities offers a sustainable solution to mitigate carbon emissions, reduce reliance on the electricity grid, and as a means of producing value-added biofuels and green chemical products. Despite challenges, these developments suggest a promising future for MES to support the transition to a decarbonised circular economy.

## Author contributions

Conceptualisation, X. N. and J. M.; investigation, X. N. and D. S.; writing – original draft, X. N.; writing – review & editing, D. S., A. B., D. W., and J. M.; validation, A. B., D. W. and J. M.; supervision, J. M.; funding acquisition, X. N., A. B., D. W. and J. M.

## Conflicts of interest

There are no conflicts to declare.

## Data availability

Data sharing does not apply to this paper, as no datasets were generated or analysed as part of this perspective.

## Acknowledgements

This work was supported by the Research Ireland National Energy Innovation Challenge Fund (EMERGE, SFI 22/NCF/EI/11268), the Sustainable Energy Authority of Ireland and Department of Agriculture, Food and the Marine under the SEAI Research, Development & Demonstration Funding Programme 2024 (EXPAND, 24/RDD/1077), and Research Ireland through the MaREI Centre for Energy, Climate and Marine (12/RC/2302\_P2 and 16/SP/3829).

## References

- 1 P. Dasgupta, *The Economics of Biodiversity: the Dasgupta Review. Abridged Version*, London, HM Treasury, 2021.
- 2 European Commission, *2020 Circular Economy Action Plan – International Aspects*, Publications Office of the European Union, 2020.
- 3 M. Crippa, D. Guizzardi, P. Federico, B. Manjola, M. Marilena and S. Edwin, *GHG Emissions of All World Countries*, Publications Office of the European Union, 2024.



- 4 M. S. Masnadi, H. M. El-Houjeiri, D. Schunack, Y. Li, J. G. Englander, A. Badahdah, J.-C. Monfort, J. E. Anderson, T. J. Wallington, J. A. Bergerson, D. Gordon, J. Koomey, S. Przesmitzki, I. L. Azevedo, X. T. Bi, J. E. Duffy, G. A. Heath, G. A. Keoleian, C. McGlade, D. N. Meehan, S. Yeh, F. You, M. Wang and A. R. Brandt, *Science*, 2018, **361**, 851–853.
- 5 Y.-I. Gao, J. Cournoyer, B. C. De, C. L. Wallace, A. V. Ulanov, M. R. La Frano and A. P. Mehta, *Nat. Commun.*, 2024, **15**, 5947.
- 6 K. Rabaey and R. A. Rozendal, *Nat. Rev. Microbiol.*, 2010, **8**, 706–716.
- 7 L. T. Angenent, I. Casini, U. Schröder, F. Harnisch and B. Molitor, *Energy Environ. Sci.*, 2024, **17**, 3682–3699.
- 8 D. A. Jadhav, K. Gunaseelan, G. T. H. Le, T. Eisa, S.-G. Park, S. Gajalakshmi, P. Gangadharan, M. A. Abdelkareem and K.-J. Chae, *J. Environ. Chem. Eng.*, 2024, **12**, 114027.
- 9 Z. Huang, R. G. Grim, J. A. Schaidle and L. Tao, *Energy Environ. Sci.*, 2021, **14**, 3664–3678.
- 10 S. Bidwai, *Caproic Acid Market Size, Share and Trends 2025 to 2034, Precedence Research*, 2025.
- 11 J. Luo, M. Pérez-Fortes, A. J. J. Straathof and A. Ramirez, *J. Environ. Chem. Eng.*, 2024, **12**, 113924.
- 12 X. Ning, R. Lin, R. O'Shea, D. Wall, C. Deng, B. Wu and J. D. Murphy, *iScience*, 2021, **24**, 102998.
- 13 K. Li, N. Hu, L. Wang, A. Zhang, Y. Bai, S. Lu, Q. Tao and F. Feng, *Int. J. Hydrogen Energy*, 2025, **103**, 851–866.
- 14 L. Liu and D. Pant, *Sustainable Energy Fuels*, 2024, **8**, 460–480.
- 15 Z. Xie, Z. Chen, X. Zheng, Y. Liu and Y. Jiang, *Int. J. Hydrogen Energy*, 2025, **103**, 528–537.
- 16 P. Dessi, L. Rovira-Alsina, C. Sánchez, G. K. Dinesh, W. Tong, P. Chatterjee, M. Tedesco, P. Farràs, H. M. V. Hamelers and S. Puig, *Biotechnol. Adv.*, 2021, **46**, 107675.
- 17 A. M. H. Putri, B. F. Ramadhoni, M. S. H. Radias, F. A. Riyadi, M. Z. Alam and Y. Muharam, *Curr. Res. Green Sustain. Chem.*, 2025, **10**, 100440.
- 18 X. Ning, C. Deng, D. T. Hickey, A. Hackula, R. O'Shea, D. M. Wall, R. Lin and J. D. Murphy, *J. Cleaner Prod.*, 2023, **423**, 138723.
- 19 W.-J. Liu, H. Jiang and H.-Q. Yu, *Energy Environ. Sci.*, 2019, **12**, 1751–1779.
- 20 S. Bolan, D. Hou, L. Wang, L. Hale, D. Egamberdieva, P. Tammeorg, R. Li, B. Wang, J. Xu, T. Wang, H. Sun, L. P. Padhye, H. Wang, K. H. M. Siddique, J. Rinklebe, M. B. Kirkham and N. Bolan, *Sci. Total Environ.*, 2023, **886**, 163968.
- 21 World Bioenergy Association, *The Global Bioenergy Statistics (GBS) Report*, 2024.
- 22 X. Zhao, H. Zhou, V. S. Sikarwar, M. Zhao, A.-H. A. Park, P. S. Fennell, L. Shen and L.-S. Fan, *Energy Environ. Sci.*, 2017, **10**, 1885–1910.
- 23 S. Babu, R. Singh, S. Kumar, S. S. Rathore, D. Yadav, S. K. Yadav, V. Yadav, M. A. Ansari, A. Das, G. A. Rajanna, O. A. Wani, R. Raj, D. K. Yadav and V. K. Singh, *Environ. Sci.:Adv.*, 2023, **2**, 1042–1059.
- 24 C. Deng, R. Lin, X. Kang, B. Wu, D. M. Wall and J. D. Murphy, *Fuel*, 2021, **306**, 121736.
- 25 X. Ning, C. Deng, X. Kang, R. O'Shea, D. M. Wall, R. Lin and J. D. Murphy, *J. Cleaner Prod.*, 2023, **426**, 139155.
- 26 X. Wu, X. Zhao, G. Yi, W. Zhang, R. Gao, D. K. H. Tang, R. Xiao, Z. Zhang, Y. Yao and R. Li, *J. Environ. Manage.*, 2024, **356**, 120604.
- 27 R. Singh, A. Goyal and S. Sinha, *Biomass Bioenergy*, 2025, **194**, 107663.
- 28 W. Ren, L. Xiong, G. Nie, H. Zhang, X. Duan and S. Wang, *Environ. Sci. Technol.*, 2020, **54**, 1267–1275.
- 29 C. Sun, T. Chen, Q. Huang, M. Zhan, X. Li and J. Yan, *Chem. Eng. J.*, 2020, **380**, 122519.
- 30 S. S. Senadheera, P. A. Withana, J. Y. Lim, S. You, S. X. Chang, F. Wang, J. H. Rhee and Y. S. Ok, *Green Chem.*, 2024, **26**, 10634–10660.
- 31 C. Deng, R. Lin, X. Kang, B. Wu, R. O'Shea and J. D. Murphy, *Renew. Sustain. Energy Rev.*, 2020, **128**, 109895.
- 32 J. Chen, J. Zhou, W. Zheng, S. Leng, Z. Ai, W. Zhang, Z. Yang, J. Yang, Z. Xu, J. Cao, M. Zhang, L. Leng and H. Li, *Sci. Total Environ.*, 2024, **946**, 174081.
- 33 J. Pan, H. Yang, L. Liu, B. Li, X. Tang, X. Wu, L. Zhang and G.-G. Ying, *Environ. Sci.:Water Res. Technol.*, 2022, **8**, 2873–2883.
- 34 G. Li, H. Yu, H. Guo, L. Wang, P. Cao and J. Shi, *Sep. Purif. Technol.*, 2025, **361**, 131319.
- 35 M. M. Mian, W. Ao, L. Xiao, J. Xiao and S. Deng, *J. Hazard. Mater.*, 2024, **478**, 135572.
- 36 X. Tian, Q. Xie, G. Chai and G. Li, *Sci. Rep.*, 2022, **12**, 5918.
- 37 M. Luo, H. Lin, Y. He, B. Li, Y. Dong and L. Wang, *Bioresour. Technol.*, 2019, **284**, 333–339.
- 38 C. Deng, R. Lin, X. Kang, B. Wu, D. Wall and J. D. Murphy, *Energy*, 2022, **239**, 122188.
- 39 Z. Zhao, H. Wu, Y. An, L. Huang and G. Zhang, *Renewable Energy*, 2025, **242**, 122458.
- 40 R. Shen, Z. Yao, J. Yu, J. Luo and L. Zhao, *Sustainable Energy Fuels*, 2022, **6**, 5324–5336.
- 41 Y. Gong, Z. Jin, X. Wang and Y. Zhang, *Water Res.*, 2025, **270**, 122845.
- 42 R. Tao, Y. Zhang, J. Yang, T. Yang, J. C. White and Y. Shen, *Environ. Sci. Nano*, 2023, **10**, 1800–1811.
- 43 Z. Zhou, E. Cui, A. A. Abid, L. Zhu, J. Xu and H. Chen, *J. Hazard. Mater.*, 2024, **477**, 135440.
- 44 A. Sokolowski, M. P. Dybowski, P. Oleszczuk, Y. Gao and B. Czech, *J. Environ. Manage.*, 2024, **371**, 123165.
- 45 F. Yang, W. Wang, Z. Wu, J. Peng, H. Xu, M. Ge, S. Lin, Y. Zeng, J. Sardans, C. Wang and J. Peñuelas, *Sci. Total Environ.*, 2024, **954**, 176300.
- 46 Y. Bai, A. Arulrajah, S. Horpibulsuk and A. Zhou, *Constr. Build. Mater.*, 2024, **442**, 137617.
- 47 R. Roychand, S. Kilmartin-Lynch, M. Saberian, J. Li and C. Q. Li, *Case Stud. Constr. Mater.*, 2025, **22**, e04233.
- 48 B. Ouyang, Z. Zhang, F. Chen, F. Li, M.-L. Fu, H. Lan and B. Yuan, *Water Res.*, 2025, **273**, 123024.
- 49 L. Zhu, B. Luo, L. Men, J. Chen, F. Xie, W. Zhang, J. Zhang and Y. Zhou, *Green Chem.*, 2025, **27**(7), 2078–2091.



- 50 A. Ratheesh, B. R. Sreelekshmy and S. M. A. Shibli, *Sustainable Energy Fuels*, 2023, 7, 1454–1465.
- 51 H. Xin, R. Yang, C. Lin, J. Zhan and Q. Yang, *Chem. Eng. J.*, 2024, **488**, 150978.
- 52 F. Sun, J. Chen, Z. Sun, X. Zheng, M. Tang and Y. Yang, *Sci. Total Environ.*, 2024, **929**, 172418.
- 53 B. A. Bregadiolli, G. M. M. Morandi Lustosa, J. V. Paulin, W. A. Bizzo, L. T. Kubota, S. Deng and T. Mazon, *Next Mater.*, 2025, 7, 100444.
- 54 Z. Ai, S. Luo, Z. Xu, J. Cao, L. Leng and H. Li, *Energy*, 2024, **313**, 133707.
- 55 L. Deng, Y. Zhao, D. Feng, W. Zhang, Y. Yu and S. Sun, *Chem. Eng. J.*, 2024, **499**, 156015.
- 56 L. Deng, Y. Zhao, S. Sun, D. Feng and W. Zhang, *Int. J. Hydrogen Energy*, 2023, **48**, 21799–21813.
- 57 J. Aslam, M. A. Waseem, X.-M. Lu, W. Sun and Y. Wang, *Chem. Eng. J.*, 2025, **505**, 159556.
- 58 Z. Yang, Z. Zou, M. A. Akhtar, W. Niu, L. Ren, S. Zhang, N. Liu and H. Cao, *J. Cleaner Prod.*, 2024, **485**, 144392.
- 59 C. Zhang, F. Ndayisenga, C. Wang and Z. Yu, *Chem. Eng. J.*, 2025, **505**, 159709.
- 60 W. Xie, B. Li, L. Liu, H. Li, M. Yue, Q. Niu, S. Liang, X. Shao, H. Lee, J. Y. Lee, M. Shao, Q. Wang, D. O'Hare and H. He, *Chem. Soc. Rev.*, 2025, **54**, 898–959.
- 61 R. Lin, C. Deng, W. Zhang, F. Hollmann and J. D. Murphy, *Trends Biotechnol.*, 2021, **39**, 370–380.
- 62 A. Elreedy, D. Härrer, R. Ali, A. Hille-Reichel and J. Gescher, *Environ. Technol. Innov.*, 2024, **36**, 103871.
- 63 J. Zhang, F. Li, D. Liu, Q. Liu and H. Song, *Chem. Soc. Rev.*, 2024, **53**, 1375–1446.
- 64 R. Xia, J. Cheng, H. Li, X. Yang, X. Ren, H. Dong, Z. Chen, X. Zhou, R. Lin and J. Zhou, *ACS Sustainable Chem. Eng.*, 2022, **10**, 2890–2902.
- 65 E. Nwanebu, M. Jezernik, C. Lawson, G. Bruant and B. Tartakovsky, *RSC Adv.*, 2024, **14**, 22962–22973.
- 66 Y. Zhu, L. Zhang, R. Gu, Y. Tian, D. Liang, W. He and Y. Feng, *Chem. Eng. J.*, 2024, **497**, 154540.
- 67 X. Ning, R. Lin, J. Mao, C. Deng, L. Ding, R. O'Shea, D. M. Wall and J. D. Murphy, *Energy Convers. Manage.*, 2024, **304**, 118245.
- 68 X. Zhong, H.-J. Peng, C. Xia and X. Liu, *J. Mater. Chem. A*, 2024, **12**, 19663–19684.
- 69 K. Cui, K. Guo, J. M. Carvajal-Arroyo, J. Arends and K. Rabaey, *Chem. Eng. J.*, 2023, **471**, 144296.
- 70 F. Harnisch and N. Xafenias, *Trends Biotechnol.*, 2024, **42**, 1035–1047.
- 71 X. Ning and N. Xafenias, *Cell Rep. Phys. Sci.*, 2024, **5**, 102262.
- 72 F. E. Liew, R. Nogle, T. Abdalla, B. J. Rasor, C. Canter, R. O. Jensen, L. Wang, J. Strutz, P. Chirania, S. De Tissera, A. P. Mueller, Z. Ruan, A. Gao, L. Tran, N. L. Engle, J. C. Bromley, J. Daniell, R. Conrado, T. J. Tschaplinski, R. J. Giannone, R. L. Hettich, A. S. Karim, S. D. Simpson, S. D. Brown, C. Leang, M. C. Jewett and M. Köpke, *Nat. Biotechnol.*, 2022, **40**, 335–344.
- 73 N. Yu, B. Bian, P. E. Saikaly, H. Zhang, K. Guo and B. E. Logan, *Chem. Eng. J.*, 2025, **519**, 165006.
- 74 G. Shang, K. Cui, W. Cai, X. Hu, P. Jin and K. Guo, *Chem. Eng. J.*, 2023, **451**, 138898.
- 75 A. Goglio, A. Carrara, H. G. E. Elboghady, M. Cucina, E. Clagnan, G. Soggia, P. De Nisi and F. Adani, *J. Power Sources*, 2025, **625**, 235623.
- 76 S. Das, V. R. S. Cheela, B. K. Dubey and M. M. Ghangrekar, *Heliyon*, 2024, **10**, e39950.
- 77 L. P. Thulluru, A. Dhanda, M. M. Doki, M. M. Ghangrekar and S. Chowdhury, *RSC Sustain.*, 2025, **3**, 471–485.
- 78 N. K. Chaitanya, A. Rajpurohit, P. S. Nair and P. Chatterjee, *Biochem. Eng. J.*, 2023, **194**, 108896.
- 79 P. Wu, J. Zhang, J. Li, Y. Zhang, B. Fu, M.-Y. Xu, Y.-F. Zhang and H. Liu, *Sci. Total Environ.*, 2023, **863**, 160898.
- 80 K. Tahir, W. Miran, J. Jang, N. Maile, A. Shahzad, M. Moztahida, A. A. Ghani, B. Kim, H. Jeon and D. S. Lee, *Sci. Total Environ.*, 2021, **773**, 145677.
- 81 J. Zhao, H. Ma, W. Wu, M. Ali Bacar, Q. Wang, M. Gao, C. Wu, C. Xia and D. Qian, *Fuel*, 2023, **332**, 126046.
- 82 Z. Zhang, J. Li, M. Ji, Y. Liu, N. Wang, X. Zhang, S. Zhang and X. Ji, *Green Chem.*, 2021, **23**, 2362–2371.
- 83 X. Ning, L. Liu, R. Lin, R. O'Shea, C. Deng, X. Xuan, R. Xia, D. M. Wall and J. D. Murphy, *Cell Rep. Phys. Sci.*, 2024, **5**, 102262.
- 84 W. Chu, Z. Wu, X. Li, M. Alvarado-Morales and D. Liang, *Renewable Energy*, 2024, **237**, 121751.
- 85 Z. Pan, X. Hu, Y. Guo, J. Yu, H. Zhang and K. Guo, *Chem. Eng. J.*, 2025, **503**, 158446.
- 86 G. T. H. Le, H. Omar Mohamed, H. Kim, K. Yoo, T. Eisa, D. A. Jadhav, H. T. T. Nguyen, H. Eam, J. Myung, P. Castaño and K.-J. Chae, *Chem. Eng. J.*, 2024, **500**, 156635.
- 87 C. Huang, Y. Chen, S. Cheng, M. Li, L. Wang, M. Cheng, F. Li, Y. Cao and H. Song, *Biotechnol. Bioeng.*, 2023, **120**, 3013–3024.
- 88 T. Zhang, H. Nie, T. S. Bain, H. Lu, M. Cui, O. L. Snoeyenbos-West, A. E. Franks, K. P. Nevin, T. P. Russell and D. R. Lovley, *Energy Environ. Sci.*, 2013, **6**, 217–224.
- 89 M. F. Alqahtani, S. Bajracharya, K. P. Katuri, M. Ali, J. Xu, M. S. Alarawi and P. E. Saikaly, *Sci. Total Environ.*, 2021, **766**, 142668.
- 90 J. Cheng, Z. Chen, R. Xia, X. Zhou, Z. Zhang, H. Dong and J. Zhou, *Energy Fuels*, 2024, **38**, 5226–5236.
- 91 J. Jack, A. Weber, S. Boltzman and S. McCord, *Environ. Sci. Nano*, 2024, **11**, 1770–1783.
- 92 F. Kracke, J. S. Deutzmann, W. Gu and A. M. Spormann, *Green Chem.*, 2020, **22**, 6194–6203.
- 93 Y. Zhang, Z. Huang, F. Qin, H. Wang, K. Cui, K. Guo, Z. Cai, X. Cai, J. Xiao, J. Carmeliet, J. Wei, Y. Song, J. Yang and L. Wang, *Nat. Chem. Eng.*, 2024, **1**, 472–482.
- 94 Y.-T. He, Q. Fu, Y. Pang, Q. Li, J. Li, X. Zhu, R.-H. Lu, W. Sun, Q. Liao and U. Schröder, *iScience*, 2021, **24**, 102163.
- 95 C. Li, Y. Liu, M. Luo, J. Cao, F. Fang, Q. Feng, J. Luo, L. Hao and C. Wang, *J. Power Sources*, 2023, **560**, 232707.
- 96 EBI, *Annual European Biochar Market Report, the European Biochar Industry Consortium*, 2024.
- 97 T. Huggins, H. Wang, J. Kearns, P. Jenkins and Z. J. Ren, *Bioresour. Technol.*, 2014, **157**, 114–119.



- 98 L. Yu, K. Seabright, I. Bajaj, D. J. Keffer, D. M. Alonso, C.-T. Hsieh, M. Li, H. Chen, S. Dai, Y. A. Gandomi, C. T. Maravelias and D. P. Harper, *Front. energy res.*, 2022, **10**, 849949.
- 99 S. Sivaraman, T. Subramaniam, S. R. Shanmugam, D. Sappani, P. Venkatachalam and N. M. C. Saady, *J. Cleaner Prod.*, 2024, **471**, 143409.
- 100 M. Roy, N. Aryal, Y. Zhang, S. A. Patil and D. Pant, *Curr. Opin. Green Sustain. Chem.*, 2022, **35**, 100605.
- 101 D. A. Jadhav, A. D. Chendake, S. Pandit, A. K. Mungray, J.-H. Jang, G. Kumar, S. Y. Al-Qaradawi, M. A. Abdelkareem and K.-J. Chae, *J. Power Sources*, 2025, **629**, 236001.
- 102 F. Enzmann and D. Holtmann, *Chem. Eng. Sci.*, 2019, **207**, 1148–1158.
- 103 P. Liang, R. Duan, Y. Jiang, X. Zhang, Y. Qiu and X. Huang, *Water Res.*, 2018, **141**, 1–8.
- 104 X. Christodoulou, T. Okoroafor, S. Parry and S. B. Velasquez-Orta, *J. CO<sub>2</sub> Util.*, 2017, **18**, 390–399.
- 105 M. Shemfe, S. Gadkari, E. Yu, S. Rasul, K. Scott, I. M. Head, S. Gu and J. Sadhukhan, *Bioresour. Technol.*, 2018, **255**, 39–49.
- 106 M. Thema, F. Bauer and M. Sterner, *Renew. Sustain. Energy Rev.*, 2019, **112**, 775–787.
- 107 D. Rusmanis, R. O'Shea, D. M. Wall and J. D. Murphy, *Bioengineered*, 2019, **10**, 604–634.
- 108 P. Battle-Vilanova, L. Rovira-Alsina, S. Puig, M. D. Balaguer, P. Icaran, V. M. Monsalvo, F. Rogalla and J. Colprim, *Sci. Total Environ.*, 2019, **690**, 352–360.
- 109 A. Lorin, D. Héleine, J. McGreer, *et al.*, *Biogenic CO<sub>2</sub> from the Biogas Industry*, European Biogas Association, Brussels, Belgium, 2022.
- 110 EBA, *European Biomethane Map 2025*, Brussels, Belgium, European Biogas Association, 2022.
- 111 European Commission, *REPowerEU, Joint European Action for More Affordable, Secure and Sustainable Energy*, Publications Office of the European Union, 2022.

